AIAA Atmospheric Flight Mechanics Conference and Exhibit
20 - 23 August 2007, Hilton Head, South Carolina

AIAA 2007-6642

ACHAB: Analysis Code for High-Altitude Balloons

Roberto Palumbo*, Michelangelo Russo†, Edoardo Filippone‡, Federico Corraro§.
CIRA, Italian Aerospace Research Centre
Flight Systems Department - Via Maiorise , 81043 Capua (CE), Italy

ACHAB is a new software tool developed to predict flight trajectory (horizontal and vertical motions) and thermal behavior of high-altitude zero pressure balloons. Its features include also ballasting and valving. This paper will describe the theoretical basis and the development process of the code, and shows an example of the possible results, that are compared with experimental flights and the outputs of a reference software tool. ACHAB was then successfully used for trajectory prediction of the Carrier system of the experimental vehicle FTB1 within the activities of the USV (Unmanned Space Vehicle) program conducted by the Italian Aerospace Research Center (CIRA). Results of this balloon flight are also analyzed and discussed in the paper.

Nomenclature

$Albedo$	=	Albedo coefficient
A_{top}	=	Balloon top projected area, m^2
A_{top0}	=	Balloon top projected area at lift-off, m^2
ASI	=	Agenzia Spaziale Italiana (Italian Space Agency)
CIRA	=	Centro Italiano Ricerche Aerospaziali (Italian Aerospace Research Centre)
C_d	=	Balloon drag coefficient
$C'_{discharge}$	=	Discharge coefficient of the venting ducts
$C''_{discharge}$	=	Discharge coefficient of the valves
c_f	=	Specific heat of the film material, J/kg/K
c_v	=	Specific heat at constant volume of the lifting gas (for Helium: 3121.5 J/kg/K)
C_{added}	=	Added mass coefficient
g	=	Acceleration of gravity, m/s^2
M_{film}	=	Mass of balloon film, kg
M_{gas}	=	Mass of lifting gas, kg
M_{load}	=	Mass of payload, kg
$M_{ballast}$	=	Total ballast, kg
p_{air}	=	Atmospheric pressure, Pa
p_0	=	Air pressure at sea level, Pa
p_{gas}	=	Gas (Helium) pressure, Pa
R_{air}	=	Specific gas constant of Air (287.05 J/kg/K)
R_{gas}	=	Specific gas constant of the lifting gas (for Helium: 2078.5 J/kg/K)
ρ_{air}	=	Air density, kg/m^3
ρ_{gas}	=	Gas (Helium) density, kg/m^3
T_{air}	=	Air Temperature, K
T_{film}	=	Balloon film bulk temperature, K
T_{gas}	=	Gas (Helium) Temperature, K
USV	=	Unmanned Space Vehicle

* Researcher, Flight System Department, E-Mail: r.palumbo@cira.it.
† Researcher, Flight System Department, E-Mail: mi.russo@cira.it.
‡ Senior Researcher, Flight System Department, E-Mail: e.filippone@cira.it.
§ Senior Researcher, Flight System Department, E-Mail: f.corraro@cira.it.

$V_{x,y,z}$ = Inertial velocity components, m/s
$V_{wind\ x,y,z}$ = Wind velocity components, m/s
$Volume$ = Balloon volume, m^3
γ = Specific heats ratio, c_p / c_v
α = Averaged balloon film absorptivity, visible sunlight
α_{IR} = Averaged balloon film absorptivity, IR
τ = Averaged balloon film transmissivity, visible sunlight
τ_{IR} = Averaged balloon film transmissivity, IR

I. Introduction

SCIENTIFIC balloons are very large flexible structures (up to 1.1 million cubic meters) that are designed to carry payloads to the upper layers of the atmosphere. The balloon systems usually consist of a balloon envelope (film), a flight chain, and the scientific payload. Scientific balloons can lift as much as 3600 kilograms to a float altitude of approximately 40 kilometers, with a flight time of hours or days (sometimes even of weeks).

Balloons are commonly used as observation platforms in studying the atmosphere. They are used more frequently than orbital satellites. Indeed, if satellites are unique in providing a global view of the Earth's atmosphere, they also suffer several limitations. In fact meteorological parameters can be observed from satellites with difficulty at stratospheric altitudes. In addition, balloon flights can be performed within a shorter time frame than that required for the development of space projects, allowing the rapid checking of new ideas, concepts, or instruments for further use in space and later for the validation of the measurements of spaceborne instruments.

The Italian Aerospace Research Centre (CIRA) is conducting an aerospace national research program named USV (Unmanned Space Vehicle), whose main objective is *designing* and *manufacturing* of two unmanned Flying Test Beds (FTB1 for atmospheric flights and FTBX for re-entry demonstrations), conceived as multi-mission flying laboratories, in order to test and verify innovative materials, aerodynamic behavior, advanced guidance, navigation and control functionalities and critical operational aspects peculiar of the future Reusable Launch Vehicle (RLV)[9].

The nominal atmospheric mission profile is based on a launch through a stratospheric balloon. For that reason, the knowledge of balloon systems and of their modeling and simulation is extremely important.

In order to fulfill this requirement, CIRA has developed the software ACHAB (Analysis Code for High Altitude Balloons) whose characteristics and performances are described in this work. Actually during the flight campaign of the first USV flying test bed (FTB1), which took place in Arbatax (Sardinia), Italy, on Feb. 24, 2007, ACHAB was successfully used for trajectory prediction of the stratospheric balloon flight.

The following Part II describes the theoretical bases of the code; Part III is about its development process, while Part IV deals with the simulation and validation procedure and reports some of the available flight data. Future developments together with the final considerations are indicated in the Conclusion paragraph.

II. Theoretical Bases

The lifting force that allows a balloon to rise derives from the Archimedes' Principle. Buoyancy strictly depends on the difference between air density and lifting gas (Helium) density and on the balloon volume. Because of the exponential decrease of pressure with altitude, the balloon expands continuously in volume during the ascent until it reaches its *float altitude*. This float altitude is a function of the payload weight, balloon volume, balloon mass, lifting gas (Helium) temperature, and atmospheric density.

The simplest concept of high-altitude scientific balloon is known as *zero-pressure* balloon. In zero-pressure balloons, large open ducts at the base of the envelope vent the excess gas so that the pressure differential from inside to outside remains small allowing the attainment of the float altitude.

In particular, during a balloon ascent, the gas inside the balloon expands until the design volume is completely filled. No further increment in altitude will then occur, except due to the upward momentum (inertia) of the system, that in turn will tend to further increase the gas volume; being the design volume already attained, this will cause the pressure inside the balloon to rise. Once a sufficient amount of pressure is built up inside, the balloon loses some of the excess gas through its venting ducts. The continued ascent, due to the upward momentum, results in a reduced air density that makes the buoyancy decrease; along with the aerodynamic drag (acting downward), this brings the balloon to stop, and hence, the resulting negative lift force causes the balloon to descend. While descending, the downward momentum of the system causes the balloon to descend below its equilibrium float altitude, resulting in a higher air density and, therefore, an increase in the lift force. This, along with the upward aerodynamic drag, causes the balloon to stop and reverse its motion. This oscillating cycle continues until the balloon loses all of its free lift

(excess gas) with decreasing amplitude due to damping caused by the aerodynamic drag force and loss of excess gas. Finally, the balloon achieves float at some altitude (Ref. 12).

For zero-pressure balloon systems, *radiative* and *convective* heat transfers between the balloon and its environment determine the temperature of the buoyant gas, which, in turn, determines its density and therefore its lifting capacity. A failure to correctly predict in-flight gas temperatures can lead to under-filling or over-filling the balloons at launch. Under-filled systems may not reach the desired float altitude. Overfilled systems will discharge lifting gas though vent ducts or even burst due to over pressurization.

In the following, the dynamical and thermal model implemented in ACHAB will be briefly summarized; they both are essentially based on what reported in Ref. 6, 8, where further details not reported here can be found, including a description of how the general geometric properties of the balloon have been modeled.

A. Dynamical Model

The forces acting on the balloon are considered to be (Fig. 1):

- buoyancy
- weight
- aerodynamic drag

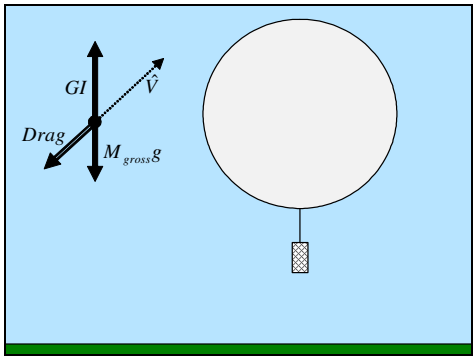

Figure 1. Forces acting on the balloon.

Buoyancy force comes from Archimedes' Principle; the total net buoyant force produced by the balloon is defined as the *gross inflation*, *GI* and is given by:

$$GI = g \cdot \rho_{air} \cdot Volume - M_{gas} g = g\left(\rho_{air} - \rho_{gas}\right) \cdot Volume \tag{1}$$

Volume is determined using the *perfect gas law*, considering the temperature value obtained by means of the thermal equations described in section B.

Weight is given by the following:

$$W = M_{gross} g \tag{2}$$

where the gross mass M_{gross} is the overall mass of the balloon (not including the gas), i.e. the sum of the payload mass, M_{load}, the ballast, and the mass of the balloon film, M_{film}. The weight of Helium instead is considered in the net buoyancy force term.

The magnitude of the **Drag** force is given by:

$$Drag = \frac{1}{2} \rho_{air} V_{rel}^2 C_d A_{top} \tag{3}$$

being the reference area the top area A_{top} as defined in Ref. 6, but appropriately projected considering the velocity direction. C_d is the drag coefficient. V_{rel} is the magnitude of the wind-relative velocity.

Hence, the differential equation governing the vertical motion, written in the NED (North – East – Down) reference frame, is the following:

$$\ddot{z} = \frac{M_{gross} g - GI + Drag_z}{M_{total}} \tag{4}$$

The total mass, M_{total}, is the sum of the gross mass, the gas mass and the *added* mass:

$$M_{total} = M_{gross} + M_{gas} + C_{added}\left(\rho_{air} Volume\right) \tag{5}$$

The *added* mass term takes into account the *added mass effect* which is caused by the acceleration of a body immersed in a fluid[6] (air, in this case).

As far as the other components (horizontal) of the motion are concerned, since no force acts horizontally except for the aerodynamic drag (in the presence of winds), the equations are simply:

$$\ddot{x} = \frac{Drag_x}{M_{total}} \qquad \ddot{y} = \frac{Drag_y}{M_{total}} \tag{6}$$

B. Thermal Model

The heat sources taken into account in this model are the following (Fig. 2):

- Direct visible Sun light
- Albedo
- Diffuse infrared radiation from ground/atmosphere
- Internal infrared self-glow of heat energy between different patches of the interior skin
- External and internal convection

In the case of nighttime flights, direct visible Sun light and albedo are, of course, not taken into account.

These heat sources are considered to be the most important ones that significantly influence the balloon flight. According to Ref. 6, to give an idea of the influences at an altitude of about 33 km on an average sunny day, the fraction of heat loads absorbed by the skin of a large scientific balloon is approximately:

Planetary surface IR	49%
Direct Solar	35%
Albedo	20%
Internal IR Self-glow	3%
Atmospheric Convection	7%

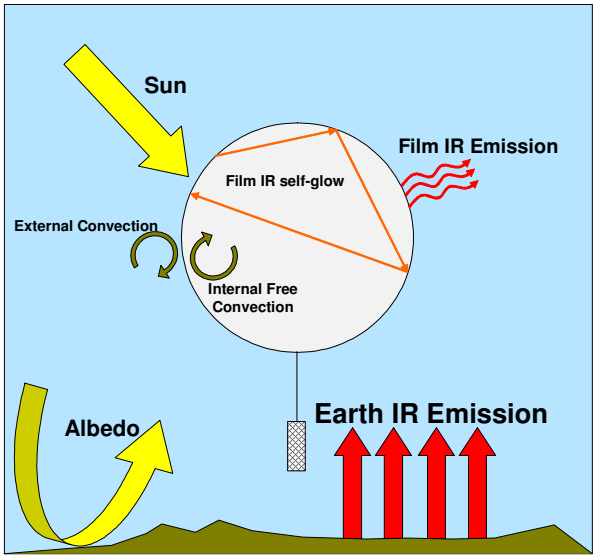

Figure 2. Heat Loads acting on the balloon.

Moreover, it is assumed that the lifting gas (Helium) is completely transparent and does not emit nor absorb: its temperature may change only as a result of the internal free convection.

The lifting gas temperature rate of change is formulated on the adiabatic expansion response modified with the *internal free convection* interaction with the film[6,8]. Considering also the hydrostatic equation and the zero-pressure assumption, it is possible to write the following equation:

$$\dot{T}_{gas} = \frac{Q_{ConvInt}}{\gamma c_v M_{gas}} - \frac{(\gamma - 1)}{\gamma} \frac{\rho_{air} g}{\rho_{gas} R_{gas}} \cdot RoC \tag{7}$$

where $Q_{ConvInt}$ is the ***Internal Convective*** *heat load,* the expression of which is based on what reported in Ref. 2, 6, 8, and RoC is the rate of climb ($RoC = -V_z$).

The rate of change of the film temperature is derived from the simple transient energy-balance equation:

$$\dot{T}_{film} = \frac{\left(Q_{Sun} + Q_{Albedo} + Q_{IREarth} + Q_{IRfilm} + Q_{ConvExt} - Q_{ConvInt} - Q_{IRout}\right)}{c_f M_{film}} \tag{8}$$

Detailed formulations of the heat fluxes[2,6,8,15,16] together with the optical surface properties of the balloon and its geometrical properties[6,8], lead to the computation of each of the heat loads present in Eq. (8):

Q_{Sun}	[*Absorbed* ***direct sun light***]	In the present model, this heat load is calculated considering the *true* solar Elevation Angle, obtained using an available algorithm (Ref. 13) that has the precision of 1 degree. This makes possible the simulation of a precise *day and night cycle* also as a function of the current latitude and longitude of the balloon. The model also takes into account the *civil twilight*[13] for the day/night transition. Finally, the atmospheric transmissivity is supposed to follow an exponential decay based on Beer's Law[8].
Q_{Albedo}	[*Absorbed* ***albedo*** *heat*]	An accurate value of the albedo coefficient (depending on the characteristics of the flight zone) must be chosen since the albedo significantly affects the thermal environment.
$Q_{IREarth}$	[*Absorbed* ***planetary IR*** *heat*]	Also this quantity is affected by the atmospheric transmissivity, calculated in a similar way as for the direct sunlight[6]. Ground emissivity characteristics and radiative surface temperature are fundamental for a correct evaluation of this heat load.
Q_{IRfilm}	[*Absorbed* ***IR self-glow***]	Trapping of heat due to multiple internal reflections also affects film temperature. These multiple reflections raise the effective interior absorption, and so, an "effective" reflectivity coefficient, r_{eff}, has to be defined[8].
Q_{IROut}	[***Emitted IR*** *energy*]	It follows the simple Stefan-Boltzmann's law, given the long-wave emissivity characteristics of the balloon film.
$Q_{ConvExt}$	[***External convective*** *heat load*]	Convection heat transfer coefficients are usually expressed in terms of the Nusselt number[2,6]. In order to determine the convective heat transfer coefficients some properties of air and Helium must be considered; more specifically, suitable expression for dynamic viscosity, conductivity and Prandtl number have been found in Ref. 6, 8 and used in the model.
$Q_{ConvInt}$	[***Internal convective*** *heat load*]	

C. Valve and Duct Flow Differential Equations

Flow through a duct or a valve depends on the differential pressure across the interface section, on the cross sectional area, on the density of gas and on a discharge coefficient.

The mass rate of change due to venting and valving is modeled with the following equation:

$$\dot{M}_{gas} = -\left(A_{duct} C'_{discharge} \sqrt{2\Delta P_{duct} \rho_{gas}} + A_{valve} C''_{discharge} \sqrt{2\Delta P_{valve} \rho_{gas}}\right) \tag{9}$$

This equation derives from Bernoulli's Equation. $C'_{discharge}$ and $C''_{discharge}$ are discharge coefficients that account for all deviations of the actual flow from the theoretical flow[8]. The discharge coefficient cannot exceed 1 and it is rarely below 0.5[8].

The pressure difference can be assessed using the hydrostatic equation[8,12], supposing that valves are usually located at the top of the balloon, while venting ducts, for the zero-pressure balloons here considered, are located at approximately 50% of the total height of the balloon.

D. Ballasting

Given a ballast discharge rate k_{ball}, the gross mass (M_{gross}) is reduced for each ballast discharge according to the following equation:

$$M_{gross} = M_{gross_{actual}} - \int_{\Delta t} k_{ball}\, dt \text{ , [kg]} \tag{10}$$

where $M_{gross_{actual}}$ is the actual gross mass before ballasting, and Δt is the discharge time interval.

III. Software Development Process

During all of its development process, the software has been constantly compared with existing data recorded from experimental flights operated by the Italian Aerospace Agency (ASI), in order to identify and investigate any discrepancy.

This analysis has been also tailored to take into account the peculiarity of the USV mission. It should be remarked that, as pointed out in the introduction and better explained in Ref. 9, for this flight the stratospheric balloon will serve as a carrier for the FTB1 vehicle, which will be dropped once reached an altitude of about 20 km: that is more than 10 km below the float altitude limit of our available balloon. The foreseen duration of the mission is below 4 h, which is much less than the time usually considered for earth observation experiments (that can last days). All this means that the analysis code has to be reliable not only in the prediction of the regime condition of the ascent flight (i.e. float altitude), but also in the first phases immediately following the lift-off.

The vertical motion of balloons depends critically on the heat transfer to and from the gas inside, because the temperature and the density of the gas determine the lift of the balloon. The balloon film plays an important role in this heat transfer mechanism, therefore its radiation properties significantly influence the performance and the vertical flight of the balloon. Yet the exact knowledge of these properties can be very challenging. Due to the large variety of film types and of film coatings, thermal radiative properties can be completely different for different balloons, giving distinct ascent characteristics to balloons. Typically, balloons are made of *polyethylene*; in this case the following Table 1 gives examples of specific heat, absorptivity (visible and IR) and transmissivity (visible and IR).

c_f [J/kg/K]	α	α_{IR}	τ	τ_{IR}
2302.7	0.07	0.02	0.885	0.842

Table 1. Polyethylene thermo-optical properties.

Another important parameter is the *Albedo* factor which is fundamental for the computation of one of the thermal loads acting on the balloon. The present model considers a constant albedo factor throughout the entire flight and, at the moment, does not account for albedo modifications due to clouds and/or possible meteorological changes in the upper atmosphere. For balloon flights over sea surfaces it has been considered a mean albedo factor of:

$$Albedo = 0.10$$

It is known that the albedo factor over the sea surface can vary remarkably especially with latitude and sun angle. According to Ref. 10, Albedo = 0.10 is a good mean value for water at latitudes around 40°N during winter (the launch site considered is Arbatax, Italy).

Another important parameter which remarkably affects the ascent flight of the balloon is the C_d. According to Ref. 4, which presents an extended literature survey on drag coefficient models for natural shape balloons, it should be reasonable to consider a variable drag coefficient during the ascent portion of the balloon flight. The arguments supporting this conclusion are essentially three:

1. inconstant shape

2. shape deformability
3. dimensional reasoning

These arguments explain why the drag coefficient cannot be exclusively dependent of the Reynolds number *Re*, but it should also be a function of the Froude number *Fr* and of another dimensionless parameter that accounts for the shape variations:

$$C_d = f(Re, Fr, L) \tag{11}$$

Therefore in this model it is suggested the following relationship for the drag coefficient:

$$C_d = 0.2\frac{k}{Fr}\cdot\left(\frac{k_1}{Re}+k_2 Re\right)\frac{A_{top}}{A_{top0}} \text{ with } k=\frac{K_{CD}}{\sqrt{A_{top0}}} \tag{12}$$

with an upper saturation value of 1.6 (Ref. 3). This relationship – with appropriate constants k_1, k_2, K_{CD} – has been found to be quite suitable to fit the flight data.

The effects of the variability of the drag coefficient on the trajectory are clearly visible in Fig. 3.

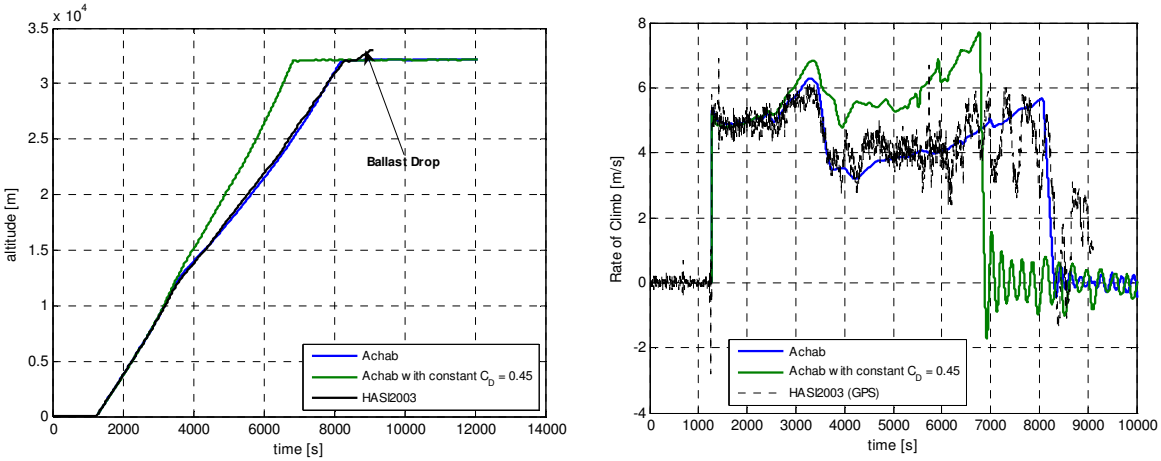

Figure 3. Comparison between ACHAB and experimental flight, for constant and variable C_D.

The balloon theoretical model so described was implemented in a computer simulation tool developed in Matlab/Simulink® environment. In order to give an idea of the possible results produced by ACHAB the outputs of an illustrative simulation for a generic balloon are shown in Fig. 4 and Fig. 5.

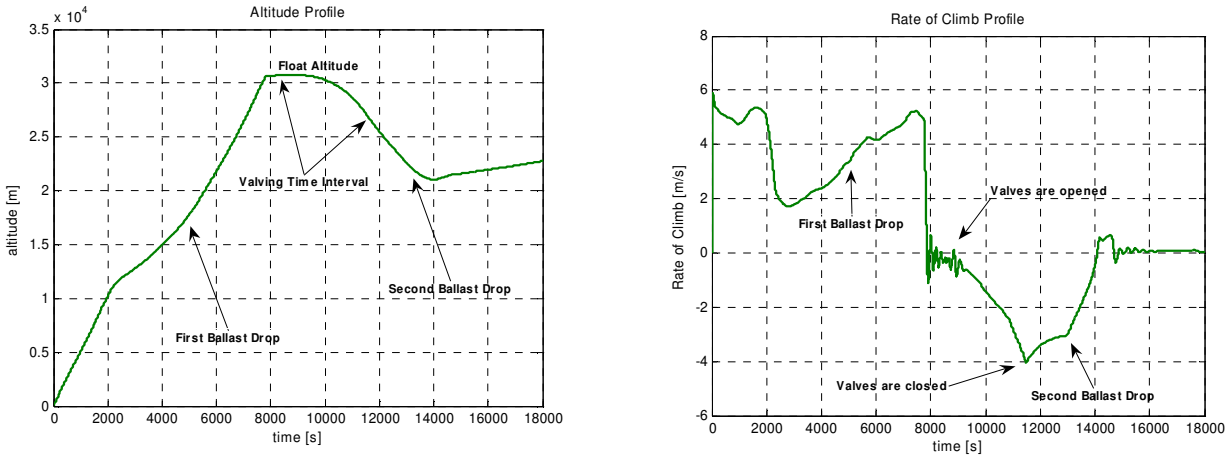

Figure 4. Results of an illustrative ACHAB simulation.

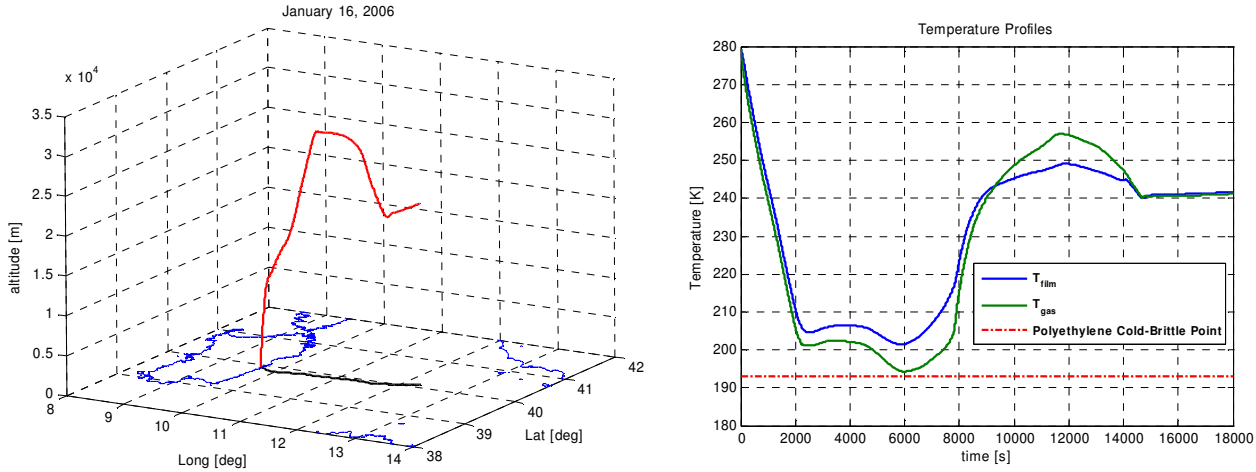

Figure 5. Results of an illustrative ACHAB simulation.

IV. Validation and Code Results

As previously explained, ACHAB has been validated comparing simulation results with GPS recorded data of different balloon flights managed by the Italian Space Agency (ASI). In particular, in the figures shown in the following, the experimental data are those of the HASI 2003 balloon flight[14].

During validation tests, ACHAB was also compared to the outputs of NASA's Scientific Balloon Analysis Model (SINBAD v3.1G). Details on the characteristics and performances of SINBAD can be found in Ref. 7, 11. It is important to point out that the definition of some input parameters in the two codes is not, of course, the same. Therefore some time has been spent in order to derive correct conversion rules to ensure the use of same simulation inputs to both models as much as possible with the purpose of making valid comparisons.

At the end of the validation process, ACHAB was considered suitable for flight prediction and was successfully used for the first USV flying test bed (FTB1) mission.

A. Validation Process

The following Fig. 6 shows an example of the comparison performed. In order to perform a more systematic evaluation of the performance of the software, different evaluation metrics have been considered, such as the integral error on the rate of climb defined as:

$$\bar{e} = \frac{1}{\Delta T}\int_{t_1}^{t_2} e(t)dt \text{ , where } e(t) = RoC_{SIMULATED}(t) - RoC_{GPS}(t) \tag{13}$$

or the *root-mean-square (rms) error* on the rate of climb.

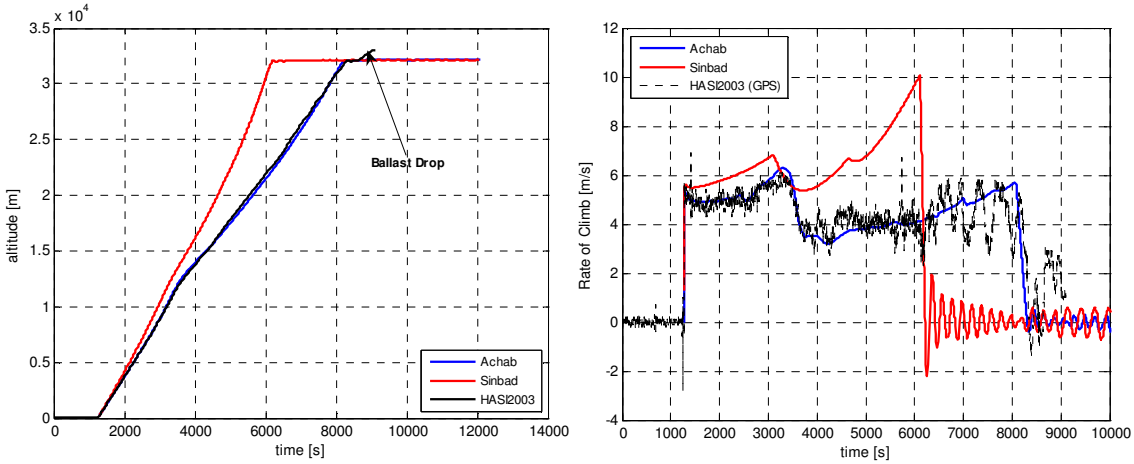

Figure 6. Comparison between ACHAB, SINBAD and experimental flight.

Table 2 shows an example of the results obtained, considering separately the portion of flight in the troposphere from that in the stratosphere (altitude > 11500 m); the whole flight is also considered defining a global error.

Error [m/s]	Simulator	Tropospheric Flight Segment	Stratospheric Flight Segment	Global Flight
$\bar{e}$	ACHAB	0.14	0.08	0.10
	SINBAD	0.87	-0.13	0.18
rms	ACHAB	0.28	1.14	0.56
	SINBAD	0.93	5.60	2.70

Table 2. Comparison between ACHAB, SINBAD and experimental flight – Errors.

B. Flight Data

ACHAB was used for trajectory prediction of the carrier system of the first USV flying test bed (FTB1) flight, which took place in Arbatax (Sardinia), Italy, on February 24, 2007. In this section some of the results are shown, together with an evaluation of the performance of the prediction.

Figure 7 shows the comparison between the actual flown trajectory of the balloon (as detected by the GPS device on the gondola) and ACHAB's prediction. In the figure, it is also shown the actual and the predicted release point of the FTB1 experimental vehicle.

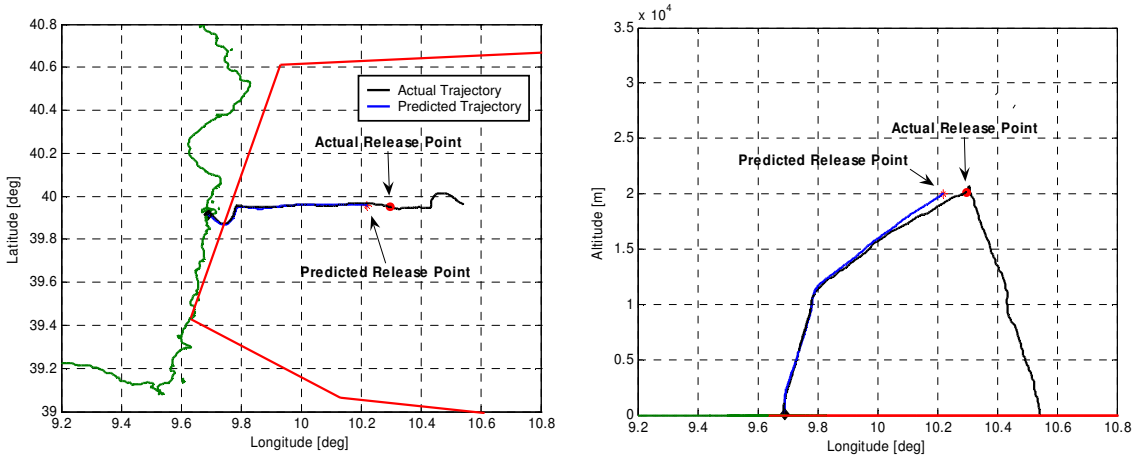

Figure 7. Comparison between ACHAB and experimental flight data.

It must be pointed out that currently, ACHAB is not able to simulate flights in non-clear sky conditions and it was validated using test cases flown on clear sky days only.

The USV-FTB1 lift-off and ascent phase occurred under *partial cloud cover*. Therefore this condition has certainly modified the thermal environment (especially long-wave radiation effects) in which the balloon moved and it may explain the difference between the actual and the predicted *release point*.

Nonetheless an evaluation of the error difference on the trajectory has shown a prediction error less than 1%.

Figure 8 shows the comparison between the actual and the predicted vertical velocity (*RoC*).

As it can be seen, vertical velocity at lift-off was underestimated. This behavior is most probably caused by an overestimation of the drag coefficient at lift-off, therefore a review and/or a fine-tuning of the drag coefficient variability law is considered necessary and will be part of the future work.

Nonetheless performance evaluation of the code has shown that ACHAB can be considered an accurate tool for balloon trajectory forecast with mean error on the *RoC* less than 0.5 m/s.

As a matter of fact, Table 3 shows the performance evaluation, considering separately the portion of flight in the troposphere from that in the stratosphere (altitude > 11500 m); the whole flight is also considered defining a global error.

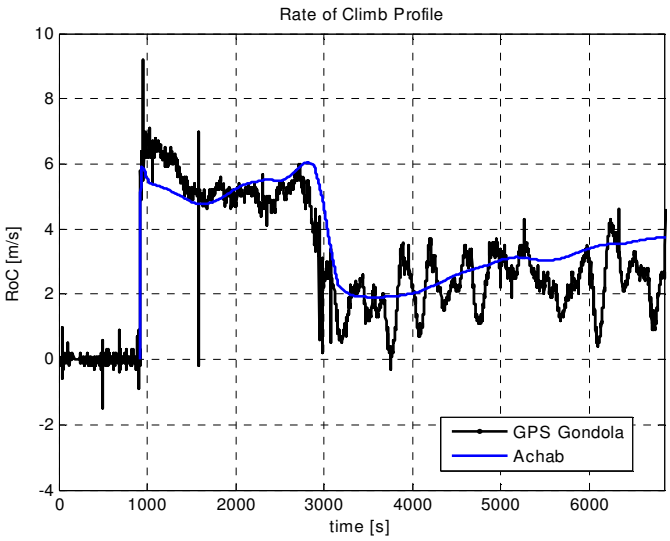

Figure 8. Comparison between ACHAB and experimental flight data.

Error [m/s]	Simulator	Tropospheric Flight Segment	Stratospheric Flight Segment	Global Flight
$\bar{e}$	ACHAB	0.12	0.54	0.38
rms	ACHAB	0.88	0.99	0.95

Table 3. Comparison between ACHAB and experimental flight – Errors.

Moreover, as it appears from Fig. 8, typical balloon oscillations in the stratospheric segment of the flight[1] are not simulated by ACHAB. Investigation and possible modelization of this phenomenon will also be considered as part of the future work.

V. Conclusion

In this paper, ACHAB, a complete software code for the analysis of the flight performance of high altitude zero-pressure scientific balloons has been presented. The availability of such a tool, and its reliability, are extremely important within the activities concerning the CIRA program USV, due to the nature of the first missions, in which the prototype of a Reusable Launch Vehicle is carried to its drop altitude by means of a stratospheric balloon.

All the theoretical fundamentals of the code have been detailed, and its performances have been analyzed by comparison with experimental flights and with a reference software tool. This comparison has shown that ACHAB is in good agreement with experimental data with a mean error on the *RoC* less then 0.5 m/s, achieving results even better than the reference software SINBAD. During the flight campaign of the first USV flying test bed, ACHAB was successfully used for flight prediction and showed an error in trajectory forecast less than 1%.

The development and the implementation of ACHAB is currently still in progress. There are several aspects concerning especially the thermal environment computation that can be modeled in a more detailed way. Among the future activities that will be conducted there are:

- Further investigation on drag coefficient variability;
- Further investigation on thermal environment modelization;
- Investigation on possible modeling of balloon buoyancy oscillations[1];
- Enhancement of the valving management system;

References

[1]Anderson, W. J., Taback, I., "Oscillation of High-Altitude Balloons", *Journal of Aircraft*, Vol. 28, No. 9, pp. 606-608.

[2]Carlson, L. A., Horn, W. J., "A Unified Thermal and Vertical Trajectory Model for the Prediction of High Altitude Balloon Performance" *Texas Engineering Experiment Station Report TAMRF-4217-81-01*, 1981.

[3]Dudley Fitz, C., Hubbard, R. R., "Determination of Coefficient of Drag for a 530,000 Cubic Foot Natural Shape Balloon", The Goddard Library: Balloon Technology Database: BT-1173, 1974.

[4]Dwyer, J. F., "Factors Affecting the Vertical Motion of a Zero-Pressure, Polyethylene, Free Balloon", Air Force Geophysics Laboratory - AFGL-TR-85-0130.

[5]Earth Orbit Environmental Heating – NASA Goddard Space Flight Center, GUIDELINE NO. GD-AP-2301.

[6]Farley, R. E., "BalloonAscent: 3D Simulation Tool for the Ascent and Float of High Altitude Balloons", *AIAA-2005-7412*, 2005.

[7]Garde, G. J., "Comparison of Two Balloon Flight Simulation Programs" *AIAA-2005-7413*, 2005.

[8]Morris, A., editor, *Scientific Ballooning Handbook* – NCAR TN/1A-99, National Center for Atmospheric Research, Boulder CO, 1975.

[9]Pastena, M. et al. "PRORA USV1: The First Italian Experimental Vehicle to the Aerospaceplane", *13th AIAA/CIRA International Space Planes and Hypersonic Systems and Technologies Conference*, Capua (Italy) 16-20/05/05, AIAA-2005-3406.

[10]Payne, R. E., "Albedo of the Sea Surface", *Journal of the Atmospheric Sciences,* Volume 29, Issue 5 (1972), pp. 959–970.

[11]Raqué, S. M., Robbins, E. J., "Recent Developments in the SINBAD Balloon Vertical Performance Model", *AIAA 94-0517*, 1994.

[12]Suwal, K. R., "An Improved Balloon Venting Model", *AIAA-1986-2430*, 1986.

[13]U.S. Naval Observatory, URL: http://aa.usno.navy.mil/

[14]HASI Balloon Flight 2003, Center of Studies and Activities for Space (CISAS), University of Padova, Italy, URL: http://cisas.unipd.it/project/hasi/balloon2003/welcome.html

[15]Stefan, K., "Performance Theory for Hot Air Balloons", *Journal of Aircraft*, Vol. 16, No. 8, pp. 539-542.

[16]Cathey, H. M., Jr., "Transient Thermal Loading of Natural Shaped Balloons", *AIAA 96-31338*, 1996.